

Flood Disaster Mapping Using Geospatial Techniques: A Case Study of the 2022 Pakistan Floods [†]

Asif Sajjad ^{1,*} , Jianzhong Lu ² , Rana Waqar Aslam ² and Muhammad Ahmad ¹

¹ Department of Environmental Sciences, Faculty of Biological Sciences, Quaid-i-Azam University, Islamabad 45320, Pakistan; muhammad380036@gmail.com

² State Key Laboratory of Information Engineering in Surveying, Mapping and Remote Sensing, Wuhan University, Wuhan 430079, China; lujzhong@whu.edu.cn (J.L.); ranawaqaraslam@whu.edu.cn (R.W.A.)

* Correspondence: asifsajjad@qau.edu.pk

[†] Presented at the 7th International Electronic Conference on Water Sciences, 15–30 March 2023;

Available online: <https://ecws-7.sciforum.net>.

Abstract: Remote sensing images are an essential tool for mapping the amount of flood inundation after flood events. For early flood estimation, flood mapping is a crucial component. This study used an integration of geospatial techniques to evaluate the flood extent in District Dera Ghazi Khan, Pakistan. The modified normalized difference water index (MNDWI) was utilized to estimate the flood extent using Landsat data. For a thorough flood investigation, pre-flood, during, and post-flood images were obtained. The analysis enabled us to delineate flood extent as well as flood duration. The result showed that the flood continued for nearly 5 weeks in the study area. This proposed geospatial technique provides a framework for the identification of inundated areas, which allows emergency responses to be focused on newly flooded areas. Hence, the current study offers a novel perspective on flood mapping and significantly contributes to flood monitoring.

Keywords: flood mapping; geospatial techniques; Landsat data; MNDWI; emergency response



Citation: Sajjad, A.; Lu, J.; Aslam, R.W.; Ahmad, M. Flood Disaster Mapping Using Geospatial Techniques: A Case Study of the 2022 Pakistan Floods. *Environ. Sci. Proc.* **2023**, *25*, 78. <https://doi.org/10.3390/ECWS-7-14312>

Academic Editor: Athanasios Loukas

Published: 3 April 2023



Copyright: © 2023 by the authors. Licensee MDPI, Basel, Switzerland. This article is an open access article distributed under the terms and conditions of the Creative Commons Attribution (CC BY) license (<https://creativecommons.org/licenses/by/4.0/>).

1. Introduction

Flood disasters are frequently occurring with more severity worldwide [1,2], and they account for more than 50% of all natural disasters that happen [3,4]. In the recent decade, flood disasters have caused over 0.25 million casualties and also registered a total of about USD 4.8 billion in economic losses [5,6]. Flooding is the primary global cause of catastrophic loss and destruction, and the number of people exposed to floods is increasing faster than the world's population [7,8].

South Asian countries, such as Bangladesh, India, and Pakistan, claim the highest number of flood-related casualties and economic losses [7,9–11]. In the recent decade, flood disasters have been common in Pakistan and have caused severe damage to all socio-economic sectors [12–14].

Floods in Pakistan generally occur in the monsoon season because of an excessive amount of rainfall in the upstream watershed of the main rivers, the Indus and the Chenab [15–17]. As a result, floods with high magnitudes have occurred in floodplain areas, which ultimately resulted in a huge impact on people's lives, property, and the overall economy of the country [18,19]. Despite the fact that this catastrophic flood menace cannot be entirely prevented, the effects can be lessened by employing effective remote sensing-based flood risk mapping [17,20]. The remote sensing technique is the most affordable way to provide extensive data on all stages of a flood disaster, which may be used for flood mapping [9,13].

Therefore, the main goal of the current research is to delineate flooded areas using suitable satellite-derived MNDWI water indices. Results from the water indices propose a step-wise approach for accurately performing flood mapping. Such an approach gives

an insight into the flood situation in this flooded area with minimum inclusion of other non-water classes. In addition, in case of flood disaster occurrence, such insights can assist in proper decision making for emergency flood management in District Dera Ghazi Khan.

Study Area

Tehsil Taunsa, District DG Khan was chosen for this study. Its geographic range is between 30.4078° N and 70.5265° E (Figure 1). It encompasses the south-western portion of Punjab and is bordered by the Punjab districts of Muzaffargarh, Layyah, and Rajanpur. The entire study area covered an area of 11,294 km² [21]. The highest and lowest rainfalls ever recorded were 50 mm in July and 2 mm in October, respectively. The average annual rainfall is 22.18 mm [22]. The locals' primary economic activity is agriculture. In the study area, cotton, sugarcane, wheat, rice, and sunflowers are the primary crops grown.

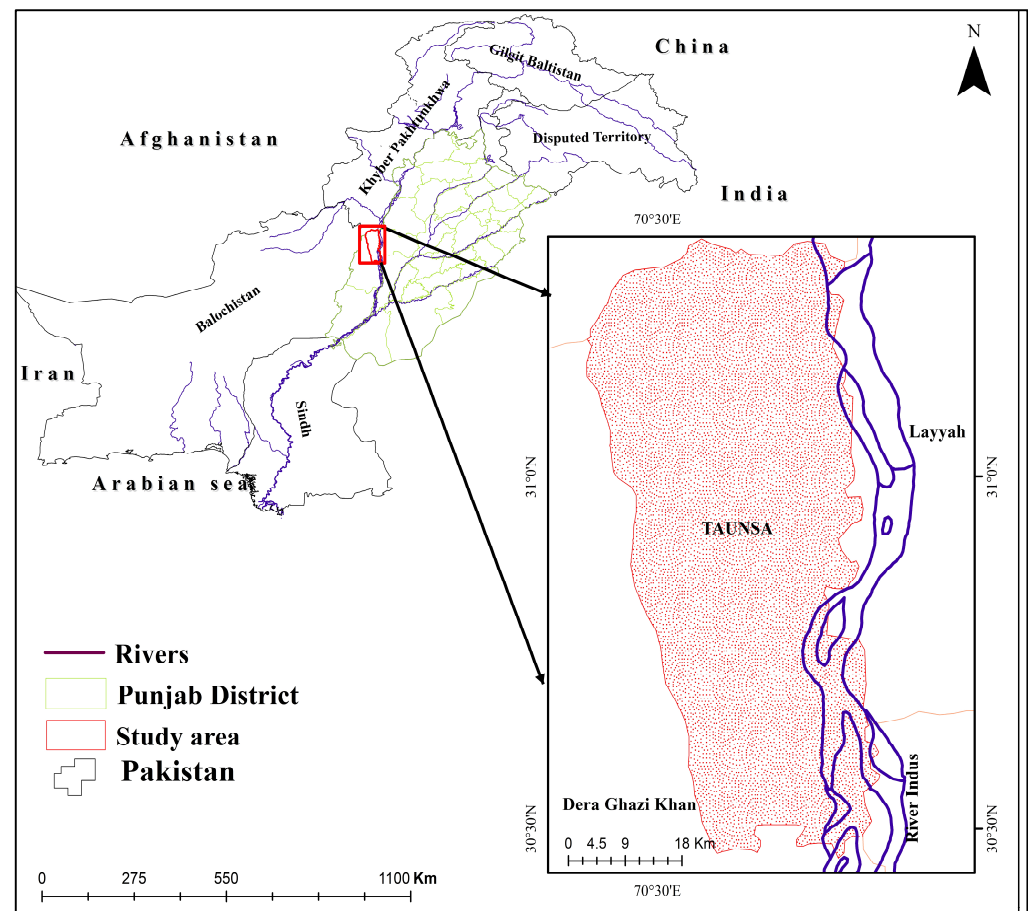


Figure 1. Location of Study Area.

2. Data and Methodology

The Landsat 8–9 OLI/TIRS data were obtained from the United States Geological Survey (USGS) [23–25]. We obtained 6 Landsat images from 21 July and 21 September 2022. Furthermore, these images were utilized to estimate MNDWI water indices for flood mapping using ArcGIS 10.8 [26,27]. This index, first presented by Xu [28], effectively calculates inundated areas. In essence, it employs the green and shortwave infrared bands to extract the flood extent, as illustrated in Equation (1):

$$\text{MNDWI} = \frac{(\text{band3}) - (\text{band6})}{(\text{band3}) + (\text{band6})} \quad (1)$$

The MNDWI index reduces accumulated noise while highlighting the water surface reflectance using the green band; the resulting values range from 1 to +1. The generated

images show negative values for built-up regions and positive values for water areas, respectively, depending on how much water area reflectance is high and how little built-up area reflectance is low in the shortwave infrared band.

Optical Landsat data, which provide up-to-date information with comparatively high temporal resolution have been widely used in the detection of flooded areas [7,17,23]. On the other hand, the presence of clouds lowers the availability of Landsat images during flooding. Certainly, synthetic aperture radar (SAR) and radar satellites can pierce clouds and obtain images in all weather situations and are commonly employed for flood mapping under these circumstances [29,30]. SAR data are normally very expensive and, in our case, the free SAR data were not available and the study area was entirely cloud-free during the 2022 flood.

3. Results and Discussion

Spatio-Temporal Flooded Area Mapping

The 2022 flood extent was identified to delineate the most inundated areas in Taunsa, Dera Ghazi Khan, Pakistan. The results show that the cumulative flood inundation from pre-flood to post-flood instances is as shown in Figures 2 and 3. The results also show that the flood inundation spans an area of approximately 526 km² in the 21 July image, whereas the highest flood inundation of 1462.24 km² can be seen in the 31 August image. Additionally, the peak flood scenario remained constant until 7 September as rain and hill torrent flow persisted from the Suleiman range and reduced flood inundation to an area of 1196 km² at a pace of 38 km²/day. On 14 September, the inundation receded to about 702 km², with a decreasing rate of 72 km²/day. Lastly, the floodwaters continued to recede and the normal stage was seen as a reducing trend persisting throughout the month of September, to the point that on September 21st, the extent of the inundation covered only 491 km² and returned to its pre-flood stage. The trend of the flood extent during three flood instances is presented in Figures 2 and 3.

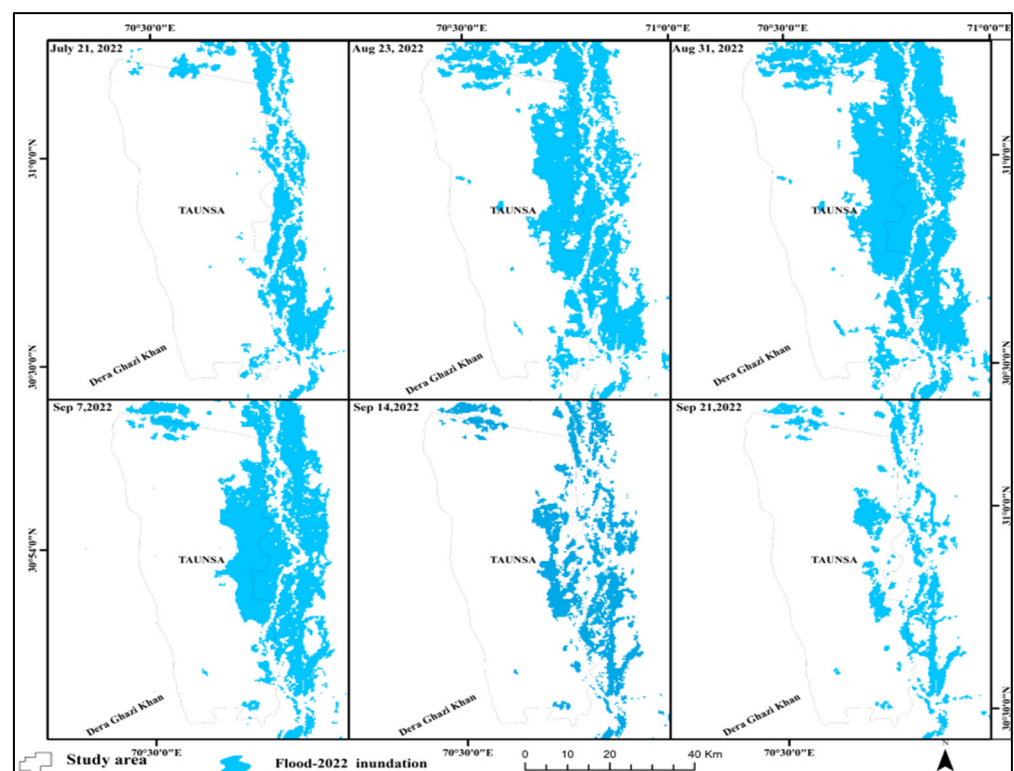


Figure 2. Temporal flood extent, peak flood extent, and duration.

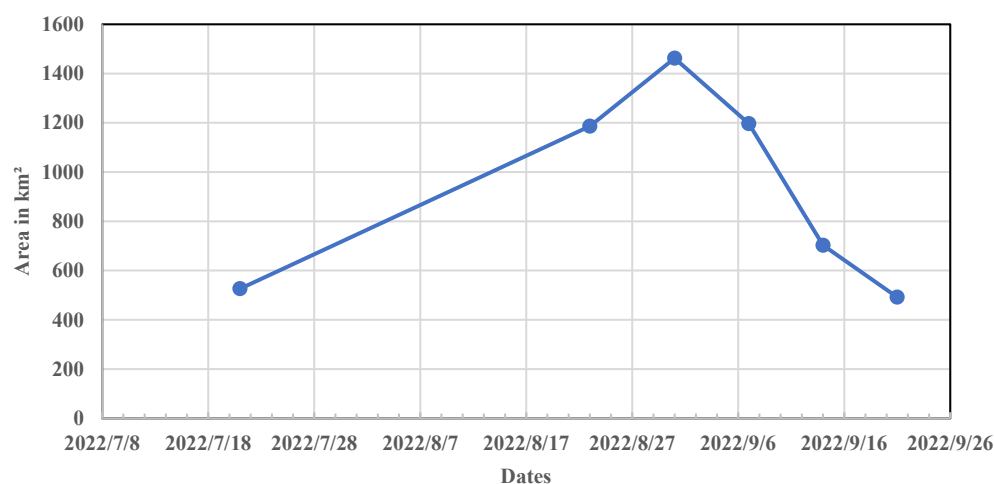


Figure 3. Temporal flood extent from during-flood (21 July to post-flood 21 September 2022).

Areas that have been flooded for several days can be detected using Landsat data [15,17,25]. Landsat data were utilized because they are also capable of accurately detecting flooded areas in built-up and agricultural areas [23,25,30]. However, to properly estimate the extent of flooding, field research and high-resolution data are required. However, due to their high cost, radar and SAR data are not used in the research area. To really observe the flooding scenario for this study, a field survey was also carried out.

As can be seen in Figures 2 and 3, the water remained in the study area for about 5 weeks after the maximum flood peak was recorded on 31 August 2022. The floodwaters subsided in two stages; during the peak stage, the water decreased gradually until the 7th of September at a rate of about 38 km² per day. Up to 21 September, the floodwaters in the moderate stage significantly decreased at a rate of 72 km² each day. The assessment of the results, however, showed that the agricultural and built-up areas suffered a great deal due to the massive inundation and duration of approximately 5 weeks.

Our results reveal that Landsat images, together with satellite-derived MNDWI indices permit detailed flooded area delineation with reliable accuracy. A recent review paper, similarly, analyzed the same indices used to depict areas under flood water and regarded MNDWI to be the most suitable in terms of its ability to differentiate between turbid water and mixed pixels [31]. Suitable satellite data are critical for flood mapping [6,9]. The temporal relationship between satellite characteristics with flood occurrence is a vital parameter in flood mapping. For example, a low-resolution moderate resolution imaging spectroradiometer (MODIS) satellite (~250 m), with its daily revisit time, has been utilized during many floods to acquire flood mapping, but with questionable accuracy [9]. However, due to the lack of during-flood SAR satellite data, such as Sentinel-1, we employed Landsat data with a resolution of 30 m for flood mapping [2,17,30]. Albertini et al. [31], in their recent review article, also concluded Landsat is the most commonly used satellite for floodwater spatial coverage detection. Despite the better spatial resolution, Landsat satellite data are constrained and cannot obtain geospatial data on time, which usually reduces their applicability to flooded area mapping [27,29]. Furthermore, the MNDWI index used achieved reliable accuracy in terms of flooded area extraction and has been efficiently used in other studies as well for detecting areas under flood water [32].

4. Conclusions

Tehsil Taunsa is particularly vulnerable to frequent riverine and hillside torrent floods. Locals living along nullahs and the Indus River deal with this flood threat almost every year. In the study region in 2022, floods produced by a two-week-long persistent wet spell occurred upstream of the Indus and in the foothills of the Suleiman range, which resulted in flooding and had a significant impact. Standing crops that were ready to be harvested, homes, animals, and all kinds of infrastructures were affected as a result.

These frequent floods are a severe problem that calls for effective preparation and impact mitigation measures, particularly through effective post-flood monitoring procedures, and particularly in Tehsil Taunsa, District D. G. Khan.

This study used remote sensing data integration and jointly employed appropriate methods to demonstrate the flood inundation severity in Taunsa. In order to estimate the inundated areas, Landsat images of flood instances were analyzed using the GIS-based MNDWI index.

The flood mapping also revealed that the flood water persisted in the study region for a month, which increased and exacerbated flood damage in the study areas. This study found that geospatial techniques can be used to carry out advanced flood mapping, which is important for flood management. As a result, the current study offers an alternative perspective on mapping flood inundation utilizing free satellite data and techniques. Flood risk mapping is the first step toward analyzing flood risk. This study can be used as a basis for further evaluating flood risk assessment and management in the study area. The methodology employed can be integrated with other radar datasets and the Analytic hierarchy process (AHP) techniques to further identify the severity of future flood risk while developing flood risk zonation.

Author Contributions: Writing—original draught, A.S.; review and editing, A.S. and J.L.; image analysis, flood inundation maps, A.S.; validation, A.S., M.A. and R.W.A. All authors have read and agreed to the published version of the manuscript.

Funding: This research received no external funding.

Institutional Review Board Statement: Not applicable.

Informed Consent Statement: Not applicable.

Data Availability Statement: The data presented in this study are available on request from the first and corresponding author.

Conflicts of Interest: The authors declare no conflict of interest.

References

1. Syvitski, J.P.; Brakenridge, G.R. Causation and avoidance of catastrophic flooding along the Indus River, Pakistan. *GSA Today* **2013**, *23*, 4–10. [[CrossRef](#)]
2. Bhatt, C.M.; Rao, G.S.; Farooq, M.; Manjusree, P.; Shukla, A.; Sharma, S.V.S.P.; Kulkarni, S.S.; Begum, A.; Bhanumurthy, V.; Diwakar, P.G.; et al. Satellite-based assessment of the catastrophic Jhelum floods of September 2014, Jammu & Kashmir, India. *Geomat. Nat. Hazards Risk* **2016**, *8*, 309–327.
3. Zhang, P.; Lu, J.; Feng, L.; Chen, X.; Zhang, L.; Xiao, X.; Liu, H. Hydrodynamic and Inundation Modeling of China's Largest Freshwater Lake Aided by Remote Sensing Data. *Remote Sens.* **2015**, *7*, 4858–4879. [[CrossRef](#)]
4. Schumann, G.; Bates, P.D.; Apel, H.; Aronica, G.T. Global Flood Hazard Mapping, Modeling, and Forecasting: Challenges and Perspectives. In *Global Flood Hazard: Applications in Modeling, Mapping, and Forecasting*; John Wiley and Sons: Hoboken, NJ, USA, 2018; pp. 239–244.
5. Mahmood, S.; Sajjad, A.; Rahman, A. Cause and damage analysis of 2010 food disaster in district Muzaffar Garh, Pakistan. *Nat. Hazards* **2021**, *107*, 1681–1692.
6. Khalid, B.; Cholaw, B.; Alvim, D.S.; Javeed, S.; Khan, J.A.; Javed, M.A.; Khan, A.H. Riverine flood assessment in Jhang district in connection with ENSO and summer monsoon rainfall over Upper Indus Basin for 2010. *Nat. Hazards* **2018**, *92*, 971–993. [[CrossRef](#)]
7. Halgamuge, M.N.; Nirmalathas, A. Analysis of large flood events: Based on flood data during 1985–2016 in Australia and India. *Int. J. Disaster Risk Reduct.* **2017**, *24*, 1–11. [[CrossRef](#)]
8. Milly, P.C.D.; Wetherald, R.T.; Dunne, K.A.; Delworth, T.L. Increasing risk of great floods in a changing climate. *Nature* **2002**, *415*, 514–517. [[CrossRef](#)]
9. Haq, M.; Akhtar, M.; Muhammad, S.; Paras, S.; Rahmatullah, J. Techniques of Remote Sensing and GIS for flood monitoring and damage assessment: A case study of Sindh province, Pakistan. *Egypt J. Remote Sens. Space Sci.* **2012**, *15*, 135–141. [[CrossRef](#)]
10. Islam, A.S.; Bala, S.K.; Haque, M. Flood inundation map of Bangladesh using MODIS time-series images. *J. Flood Risk Manag.* **2010**, *3*, 210–222. [[CrossRef](#)]
11. Gaurav, K.; Sindha, R.; Panda, P.K. The Indus flood of 2010 in Pakistan: A perspective analysis using remote sensing data. *Nat. Hazards* **2011**, *59*, 1815–1826. [[CrossRef](#)]
12. Hashmi, H.N.; Siddiqui, Q.T.M.; Ghuman, A.R.; Kamal, M.A.; Mughal, H. A critical analysis of 2010 floods in Pakistan. *Afr. J. Agric. Res.* **2012**, *7*, 1054–1067.

13. Mahmood, S.; Rahman, A.; Sajjad, A. Assessment of 2010 flood disaster causes and damages in district Muzaffargarh, Central Indus Basin, Pakistan. *Environ. Earth Sci.* **2019**, *78*, 63. [[CrossRef](#)]
14. Sajjad, A.; Lu, J.; Chen, X.; Chisenga, C.; Mahmood, S. The riverine flood catastrophe in August 2010 in South Punjab, Pakistan: Potential causes, extent and damage assessment. *Appl. Ecol. Environ. Res.* **2019**, *17*, 14121–14142. [[CrossRef](#)]
15. Sajjad, A.; Lu, J.; Chen, X.; Chisenga, C.; Saleem, N.; Hassan, H. Operational Monitoring and Damage Assessment of Riverine Flood-2014 in the Lower Chenab Plain, Punjab, Pakistan, Using Remote Sensing and GIS Techniques. *Remote Sens.* **2020**, *12*, 714. [[CrossRef](#)]
16. Naeem, B.; Azmat, M.; Tao, H.; Ahmad, S.; Khattak, M.U.; Haider, S.; Ahmad, S.; Khoro, Z.; Goodell, C.R. Flood Hazard Assessment for the Tori Levee Breach of the Indus River Basin, Pakistan. *Water* **2021**, *13*, 604. [[CrossRef](#)]
17. Sajjad, A.; Lu, J.; Chen, X.; Chisenga, C.; Mazhar, N.; Nadeem, B. Riverine flood mapping and impact assessment using remote sensing technique: A case study of Chenab flood-2014 in Multan district, Punjab, Pakistan. *Nat Hazards* **2022**, *110*, 2207–2226. [[CrossRef](#)]
18. National Disaster Management Authority((NDMA). *Annual Flood Report*; Regional Office: Islamabad, Pakistan, 2021.
19. Punjab Provincial Disaster Management Authority (PPDMA). *Annual Flood Report*; Regional Office: Lahore, Pakistan, 2021.
20. Siddiqui, M.; Haider, S.; Gabriel, H.F.; Shahzad, A. Rainfall–run off, flood inundation and sensitivity analysis of the 2014 Pakistan flood in the Jhelum and Chenab River basin. *Hydrol. Sci. J.* **2018**, *63*, 13–14. [[CrossRef](#)]
21. Federal Flood Commission Islamabad (FFCI). *Annual Flood Report*; Ministry of Water and Power, Government of Pakistan: Islamabad, Pakistan, 2021.
22. Pakistan Meteorological Department (PMD). *Annual Report*; Regional Meteorological Observatory: Lahore, Pakistan, 2022.
23. Munasinghe, D.; Cohen, S.; Huang, Y.F.; Tsang, Y.P.; Zhang, J.; Fang, Z.F. Intercomparison of Satellite Remote Sensing-Based Flood Inundation Mapping Techniques. *J. Am. Water Resour. Assoc.* **2018**, *54*, 834–846. [[CrossRef](#)]
24. Revilla-Romero, B.; Hirpa, F.A.; Pozo, J.T.; Salamon, P.; Brakenridge, R.; Pappenberger, F.; De Groeve, T. On the use of global flood forecasts and satellite-derived inundation maps for flood monitoring in data-sparse regions. *Remote Sens.* **2015**, *7*, 15702–15728. [[CrossRef](#)]
25. Shen, L.; Li, C. Water body extraction from Landsat ETM+ imagery using adaboost algorithm. In Proceedings of the IEEE 2010 18th International Conference on Geoinformatics, Beijing, China, 18–20 June 2010; pp. 1–4.
26. Alphan, H.; Doygun, H.; Unlukaplan, Y.I. Post-classification comparison of land cover using multitemporal Landsat and ASTER imagery: The case of Kahramanmaraş, Turkey. *Environ. Monit. Assess.* **2009**, *151*, 327–336. [[CrossRef](#)] [[PubMed](#)]
27. Rokni, K.; Ahmad, A.; Selamat, A.; Hazini, S. Water feature extraction and change detection using multitemporal Landsat imagery. *Remote Sens.* **2014**, *6*, 4173–4189. [[CrossRef](#)]
28. Xu, H. Modification of normalized difference water index (NDWI) to enhance open water features in remotely sensed imagery. *Int. J. Remote Sens.* **2006**, *27*, 3025–3033. [[CrossRef](#)]
29. Uddin, K.; Matin, M.A.; Meyer, F.J. Operational Flood Mapping Using Multi-Temporal Sentinel-1 SAR Images: A Case Study from Bangladesh. *Remote Sens.* **2019**, *11*, 1581. [[CrossRef](#)]
30. Notti, D.; Giordan, D.; Caló, F.; Pepe, A.; Zucca, F.; Pedro Galve, J. Potential and Limitations of Open Satellite Data for Flood Mapping. *Remote Sens.* **2018**, *10*, 1673. [[CrossRef](#)]
31. Albertini, C.; Gioia, A.; Iacobellis, V.; Manfreda, S. Detection of Surface Water and Floods with Multispectral Satellites. *Remote Sens.* **2022**, *14*, 6005. [[CrossRef](#)]
32. Güvel, Ş.P.; Akgül, M.A.; Aksu, H. Flood inundation maps using Sentinel-2: A case study in Berdan Plain. *Water Supply* **2022**, *22*, 4098–4108. [[CrossRef](#)]

Disclaimer/Publisher’s Note: The statements, opinions and data contained in all publications are solely those of the individual author(s) and contributor(s) and not of MDPI and/or the editor(s). MDPI and/or the editor(s) disclaim responsibility for any injury to people or property resulting from any ideas, methods, instructions or products referred to in the content.